PROCEEDINGS, 46th Workshop on Geothermal Reservoir Engineering
Stanford University, Stanford, California, February 15-17, 2021
SGP-TR-218

The Review of Worldwide Geothermal Top of Reservoir with JIWA T.o.R

Muhammad Fahran Fauzan Tandipanga[1], Annisa' Amalia[1], Chelsea Castro[2], Muhammad Sidqi[3], Jantiur Situmorang[3]

1. Universitas Gadjah Mada, Bulaksumur, Caturtunggal, Kec. Depok, Kabupaten Sleman, Daerah Istimewa Yogyakarta, Indonesia

2. Institut Teknologi Bandung, Jl. Ganesha No.10, Lb. Siliwangi, Bandung, West Java, Indonesia

3. AILIMA, CIBIS Business Park, TB Simatupang, Jakarta, Indonesia

fahranfauzan@mail.ugm.ac.id

Keywords: Top of reservoir, Base of Conductive, BPD, Geothermometer, drilling, exploration drilling, JIWA

ABSTRACT

JIWA Top of Reservoir (T.o.R.) is a new analytic tool introduced by AILIMA to estimate the geothermal T.o.R. uncertainties in the exploration phase. This tool is tested in this research by employing the exploration data from geothermal fields around the world to simulate geothermal T.o.R estimation prior to exploration drilling.

1. INTRODUCTION

Recognizing the uncertainties of geothermal top of reservoir (T.o.R) depth during the exploration phase is pertinent in designing well prognosis for the drilling team to anticipate when managing a drilling activity of an exploration well, particularly, the decision to set the depth of production casing shoe. It is crucial to determine the depth of the production casing rightly to prevent costly geothermal drilling problems from occurring. However, rightly setting up the casing for the first drilling activity is immensely harder compared to subsequent drilling activities, since it relies on a lot of presumption that should be as representative as possible to the expected depth. Hole (2008) further affirmed that the utilized assumption should depict the subsurface lithology and fluid conditions for the total drilled depth as close as possible. Utilized presumption should ensure that the production casing reaches the minimum depth required to isolate incoming fluid from the colder formation. Moreover, the production casing also should not be set too deep to prevent geothermal performance's disruption that affects the total cost and successful deliverability.

To resolve the problem, AILIMA produces an analytical tool in JIWA Cloud Computing Systems called JIWA T.o.R. This user-friendly tool is aimed to be a platform for the subsurface team and related expertise to collaboratively estimate the T.o.R depth uncertainties during exploration drilling. The embedded Monte Carlo algorithm and dynamic features within the system deliver the result in a probabilistic manner to enhance the T.o.R approximation to be as representative as possible to reduce drilling risks.

The purpose of this paper is to review the top reservoir of drilled wells in the convective geothermal systems around the world using JIWA T.o.R and compare the result with the actual top of the reservoir information obtained from published literature.

2. LITERATURE STUDY

2.1 Geothermal Exploration Drilling

Prior to the geothermal development, there are various processes that are followed. The exploration drilling commences as sure as the geological, geophysical, and geochemical (3G) surveys have been conducted and obtained data has been interpreted. These exploratory wells are required to study the resources characteristic, including the temperature, permeability, and fluid chemistry of the target (Axelsson and Franzson, 2012).

The challenges of the geothermal reservoir made this stage is quite costly due to various challenges and risks are mostly associated with temperature, permeability, and fluid chemistry (Hadi et al., 2010). The uncertainties on those aspects are strongly related to the drilling risks, especially on setting the right casing design. The right casing design is one of the most critical aspects of exploration drilling, including the selection of casings, casing specification and casing shoe depths (Hole, 2008).

2.2 Setting Casing Depth as One of The Biggest Risk in Drilling Exploration Wells

Appropriately setting up the casing design holds the highest precedence in reducing geothermal drilling risks. The information pertains to casing design, such as the number of the casing string, their diameters and length, and wall thickness are specified by the casing program (Hossein-Pourazad, 2005). This information derives from the estimation of the total depth, well target and potential drilling problems like lost circulation zone and lithology, and how the casing shoe should be set in the impermeable zone. These particulars serve as several preliminary well design objectives should be prepared prior to the drilling program.

Designing the casing running procedure is the most arduous part of the drilling program. It is immensely difficult mainly due to a significant number of design variables required for casing design possess their own associated degree of uncertainty. Moreover, the impact of each design is often not well-understood, resulting in either under-design or over-design occurrences (Mason et. al., 2003). Design pitfalls principally figure on rightly setting up the casing. Rightly setting the casing for first drilling is considerably harder compared to subsequent drilling activities since it relies on a lot of presumption that should be as close as possible to the expected depth.

In navigating through potential complications, the casing depth should be determined at the right depth. Hossein-Pourazad (2005) noted the depth of the production casing is determined to prevent deep fluids from the colder formations invading the well. The utilized initial assumption should be as representative as possible to the subsurface lithology and fluid conditions for the total drilled depth (Hole, 2008). One of the main determinants, however, has to do with minimum depth for safety reasons. The production casing shoe is set at the top of the reservoir to isolate it from cold aquifers because they can cause difficulties in initiating the flow of geothermal fluid through the well due to a substantial pressure drop (Sarmiento, 2007).

2.3 How to Reduce The Risks of Drilling in The Exploration Phase Associated with The T.o.R Uncertainties?

One of the challenges of the geoscience data interpretation to determine the casing depth is the inherent problem of high-uncertainties of subsurface geological and engineering data and analysis. During the exploration phase, multidimensional data is collected by different people at different times and different scales – before it gets merged together into a singular, final interpretation that includes many assumptions (Zabalza-Mezghani et al., 2004). According to Paté-Cornell (1996), these assumptions yield uncertainties to the final interpretation in the form of epistemic uncertainty and aleatory variability. Epistemic uncertainty results from lack of knowledge and can be overcome through the collection of more data. Aleatory variability, however, is unpredictability due to inherent randomness (Witter et al., 2019). Aleatory variability is also a function of scale that influences unpredictability in the geological aspects of a geothermal site, which later increases TOR uncertainties and further, affects the decision-making within the drilling plans.

Resolving aleatory variability is definitely a lot more challenging but imperative in reducing drilling risks. In this paper, we integrate Trainor-Guitton et al (2017) methodology with Monte Carlo principle to generate an estimate of the overall uncertainty in the prediction due to all uncertainties in the variables (Kalos and Whitlock, 2008). This approach characterizes the uncertainty for any nonlinear random function f from several T.o.R interpretations derived from the magnetotelluric (MT) or resistivity-based surveys. Deterministic approach is not utilized despite its ability to pinpoint a singular value due to its inability to deliver the uncertainty required in well plans, hence reducing the T.o.R depth accuracy required for determining the casing depth. Conversely, Monte Carlo simulation in quantifying uncertainty to a specific T.o.R depth range can be utilized for well planning and map its strength, weaknesses, and pitfalls (Adams et al., 2009). This approach allows people to understand risk and opportunity in improving decision making consideration.

To quantify T.o.R uncertainties utilizing Monte Carlo simulation, iteration is necessary to obtain successively closer and more accurate approximation (Adomian and Malakian, 1980). Furthermore, iteration ensures that the yielded estimates fulfil a specific confidence interval. In this paper, we utilized 10,000 as the number of iterations for each field’s simulation to estimate the TOR uncertainties.

2.4 Base of Conductive (B.o.C)

T.o.R uncertainties can be further constrained starting with reducing the uncertainties of the base of conductive, meaning the estimated B.o.C elevation is as close as possible to the top of the reservoir. Base of conductive (B.o.C) refers to the base of low permeability zone, generally in the form of a smectite clay cap in the geothermal system. Smectite clay cap is characterized by low resistivity (1-10 ohm.m) due the high cation exchange capacity (CEC) of smectite (Usher et al., 2000). Dyaksa et al. (2016) observed that B.o.C is correlated with a temperature around 180-220^{0}C. based on the studies from the developed fields such as Salak, Darajat and Wayang Windu. Research from Anderson et al. (2000) also mentioned that the base of conductive is corresponding to the range. The B.o.C smectite clay zone elevation is a significant aspect of most geothermal MT interpretation since this zone usually conforms to the top of the reservoir (Cumming et al. 2010).

The depth to the base of B.o.C roughly corresponds to the base of the smectite alteration zone. However, the other types of impermeable cap exist (Cumming, 2016). Dyaksa et al (2016) also reported how the presence of the mixed layer smectite-illite in Rantau Dadap and Muara Laboh geothermal field that can not be mapped as the conductive layer due the high resistivity before exploration drilling. The other type of impermeable cap also noted by Gunderson et al. (2000) in Awibengkok geothermal field, smectite-rich hydrothermal eruption debris flow is found across the reservoir that cannot be observed by the MT but was detected by the time-domain electromagnetic (TDEM).

Cumming (2016) figured out that the composition of the rock can affect the claycap forming. Low magnesium volcanic rocks, such as trachyte and phonolite lavas and tuff, typically contain less low resistivity smectite, but not as low as the 2 to 10 ohm-m typical in andesites and basalts. In addition, meteoric water can provide enough magnesium to support the abundant smectite in very porous trachyte and phonolite tuffs formation. As the conclusion, the interpretation of resistivity is complicated due the variation of the clay cap composition in volcanic prospect, particularly a resistivity with a particular isotherm (Cumming, 2016).

The uncertainty of the MT interpretation can be reduced by using a MeB method after drilling, the results can facilitate revisions of conceptual models, well targeting plans that were based on resistivity surveys, and well casing decisions that depend on formation temperatures. (Gunderson et al., 2000).

2.5 Reservoir Temperature

Another parameter input that corresponds to the T.o.R estimate is the width uncertainty of the expected reservoir temperature. The actual reservoir temperature obtained from the temperature profile after the well completion. Until exploration drilling, however, the temperature isothermal profile is highly uncertain. Geothermometer becomes the important exploration tool to estimate the subsurface temperature of a geothermal prospect area before any deep wells are drilled. Geothermometer is very useful, particularly in the exploration and development phases. Chemical geothermometers (solute and gas geothermometer) are the most used geothermometers that depend on the mineral-fluid equilibrium preserved during the passage of fluid to the surface (Yock, 2009). The calculation of subsurface temperatures from geochemical analyses of water and steam collected at hot springs, fumaroles, geysers, and shallow water wells is a standard tool of geothermal exploration. The calculation of chemical geothermometers rests on the assumption that some relationship between chemical or isotopic constituents in the water was established at higher temperatures and this relationship persists even after the water cools as it flows to the surface.

The other type of geothermometers is mineral geothermometer, usually using a proportion of the clay minerals, such smectite illitization. However, as mentioned by Essene and Peacor (1995), clays mineral systems cannot be used as accurate thermometers since stabilities of clay minerals are unlikely to attain equilibrium at low temperatures.

2.6 Boiling Point to Depth (BPD)

The BPD pressure profile is that of a static water column whose temperature, at local pressure saturation, is everywhere (Figure 1). The approximation of BPD means that the saturation of steam is near to residual. BPD is useful for many purposes, a good approximation of the initial state of the upflowing core of the reservoir. However this is only an approximation, pressures and temperatures can be higher or lower, and it is incorrect to regard BPD as any sort of theoretical maximum temperature (Grant, 2011).

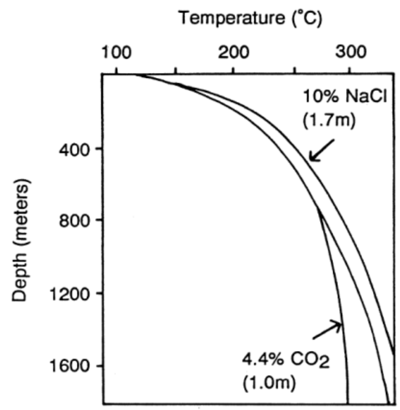

Figure 1: Boiling point to depth (Nicholson, 1993)

2.7 Acquiring T.o.R Information from Well Data

In geothermal drilling, the actual top of reservoir information could be determined from several well data, preferably the pressure-temperature (PT) profile. The PT static data is carried out during drilling of wells, during heating-up after drilling using temperature and pressure logging tools. The data is monitored over a period of time to understand the natural thermal state of the reservoir. The temperature profile will indicate the convective zone as the zone with the linear temperature while the pressure profile will indicate the convective zone by the increasing pressure, as the high pressure shows the recharge zone (upflow zone) and together will be indicating the top of the reservoir within a well (Steingrímsson, 2013).

Other types of well data which are able to be used to indicate the actual top of the reservoir are drilling parameters, such as lost circulation or the presence of the first euhedral epidote. The loss circulation indicates intersecting fractures or permeable zones, which are commonly found in geothermal reservoirs (Makuk, 2013). The first euhedral epidote, on the other hand, can also be used to signify the high temperature and permeable zone, which is also commonly found in reservoir zones (Omenda, 1993; Gylfadóttir et al., 2011). However, pressure-temperature profile is the most reliable data used to confirm the actual top of the reservoir.

2.8 How JIWA T.o.R. Can Help?

JIWA Top of Reservoir (T.o.R.) is one of the analytics tools that are provided in JIWA dashboard. This user-friendly tool is aimed as a platform for geophysicists, geochemists, geologists, and reservoir engineers to collaboratively estimate the top of the reservoir prior to the exploration drilling. JIWA T.o.R. can be utilized for the type of convective geothermal field and mainly controlled by magmatism. The input encloses the base of conductive parameters, which is related to the presence of clay cap layer and mainly affected by hydrothermal alteration. Further introduction of JIWA T.o.R. has been elaborated in Sidqi et al (2021). This research will mainly focus on the application of JIWA T.o.R. in determining the worldwide fields' top of the reservoir. The output provided from this software in form of range is a proper approach to constrain the uncertainties from the input, therefore the risk in each well can be conceived properly.

3. METHOD

A total of twenty geothermal fields, including forty-one wells worldwide are reviewed from data derived from published and reputable sources. The review covers convection geothermal play with magmatic control or also known as a convective hydrothermal system (Muffler, 1993). It is identified by the presence of a conductive layer of rock adjacent to the reservoir zone, referred to as claycap.

The T.o.R.information inferred from the well data is a primary priority at data collection, in order to compare and evaluate the output from the software. The pressure-temperature profile becomes the main reference for this research. If it's not available or less reliable due to the unknown condition, such as situated in other than natural state condition, the attested conceptual model which has considered the pressure-temperature profile is used as the alternative. However, if those data are not found, the mineralogy (first euhedral epidote appearance) or loss circulation (total or partial) data will be the last alternative.

B.o.C information is mainly taken from the cross-section of the MT or other type of resistivity model which has well trajectory information. The delineation of B.o.C elevation uses the range of resistivity value of 5-10 ohm.m, while the temperature of B.o.C is using the range of 180-220^{0}C. The explanation from these ranges have been explained in the previous section of this research. The uncertainties of this information is covered with the probabilistic input using the rectangular distribution to cover the uncertainty of B.o.C elevation. For several special cases such as in the Rotokawa field, the B.o.C is delineated in higher resistivity values, adjusted with the subsurface interpretation of its sources. In several cases, the resistivity model did not enclose trajectory information well, so the B.o.C information is obtained from attested conceptual models which attach this information.

The first approach to reservoir temperature is using the boiling chloride spring in the form of silica geothermometer. The second approach, if the data availability of boling chloride spring is not sufficient (horizontal distance from the targeted well, etc) the cation type of geothermometer is used. The third approach is using fumarole and analyzed with a gas geothermometer. The last approach is using the well temperature's data.

After all of the data is collected and validated, the input process is done in JIWA T.o.R. software. The algorithm used in this software is based on a boiling point-to-depth (BPD) plot that has been explained by Sidqi et al (2021). The output provided by this software is available in form of depth chart, histogram, and percentile table, with terminology of P1 (1st percentile), P10 (10th percentile), P20 (20th percentile), and so on until P99 (99th percentile). The output is therefore visualized in the next section of this paper.

The visualization of the result is presented in several types of charts. The percentile of distribution at each well is presented in a bar chart **(Fig. 6**) and the frequency of each percentile (**Fig. 7**). The depth uncertainty to analyze the correlation between data input type and the calculated top of reservoir is shown at **Fig. 5**, while the cumulative frequency curve of calculated T.o.R. depth range is presented at **Fig. 8**. Sensitivity analysis by correlating the base of conductive and temperature estimates uncertainty with uncertainty obtained from JIWA T.o.R system is shown at **Fig. 9** and **Fig.10.**

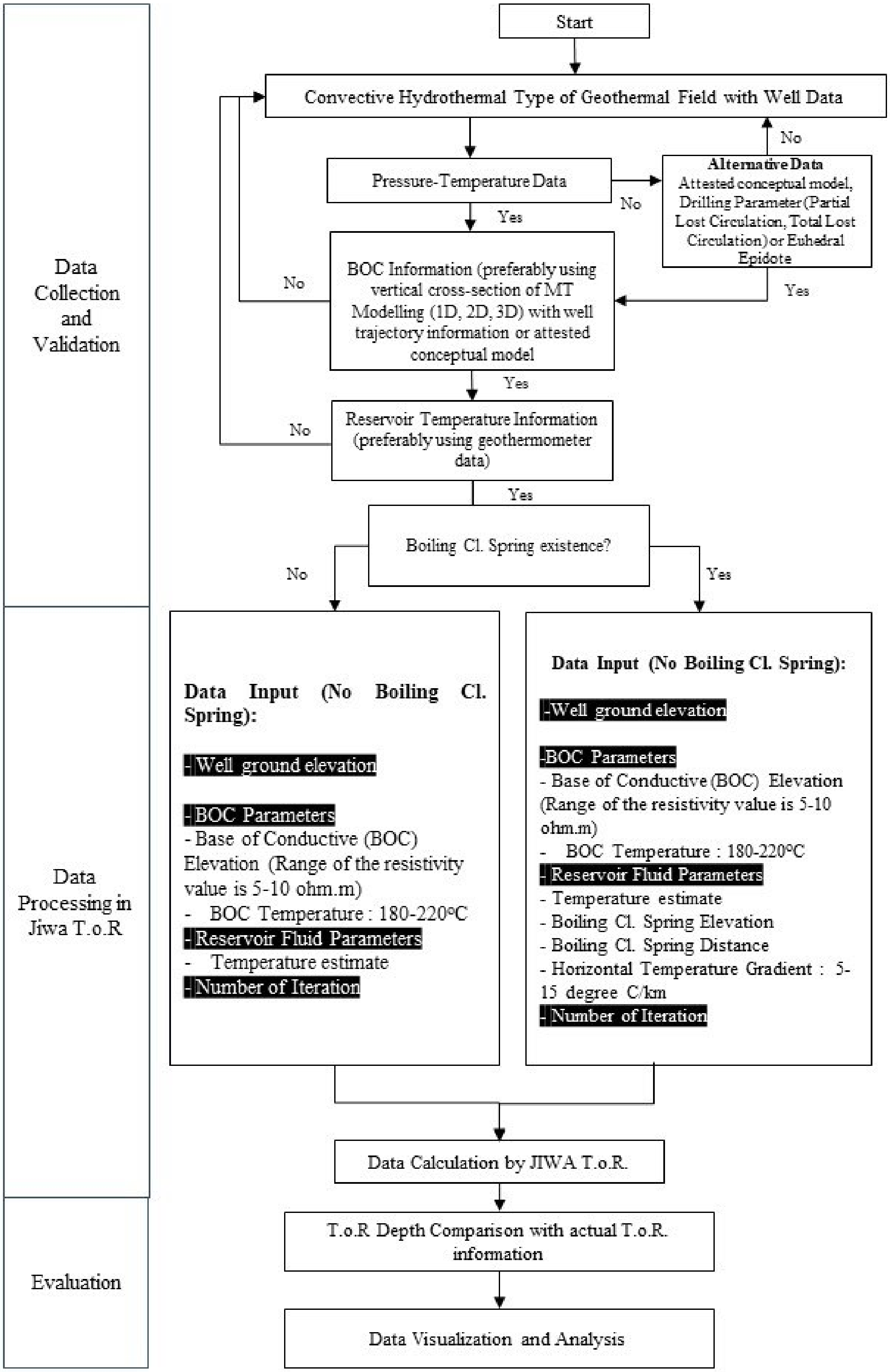

Figure 2: Flowchart of the research.

4. FIELD DATA

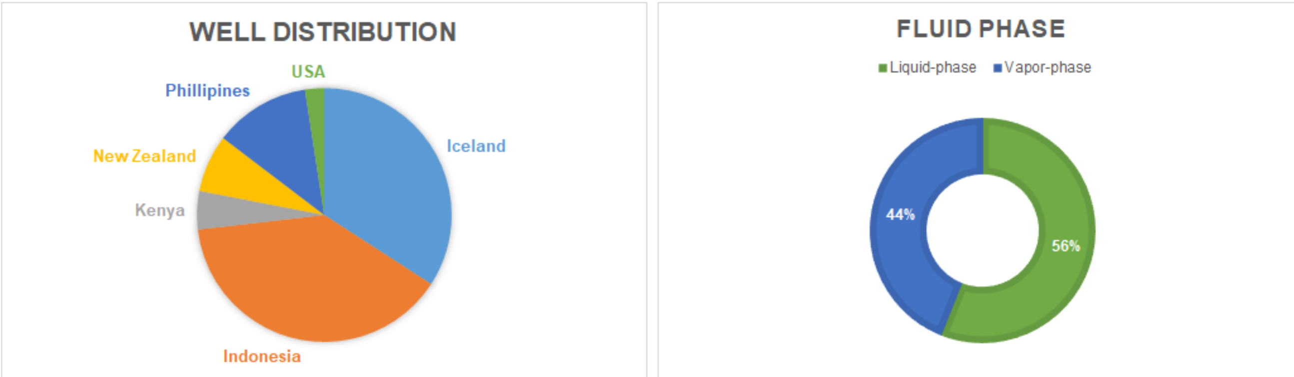

Figure 3: Worldwide distribution of utilized well information.

A total of twenty geothermal fields and forty-one geothermal wells have been studied from published literature. Data was obtained from perusing various open-access publications to obtain the information of the base of the conductive layer, primarily interpreted from available, high-resolution MT or resistivity profiles (Figure 3). To determine the actual top of reservoir depth, the pressure-temperature diagrams or conceptual model are primarily utilized, and in case it is not available, the record of the first euhedral appearance (epidote), PLC (partially lost circulation), or TLC (total lost circulation data) are utilized as alternative.

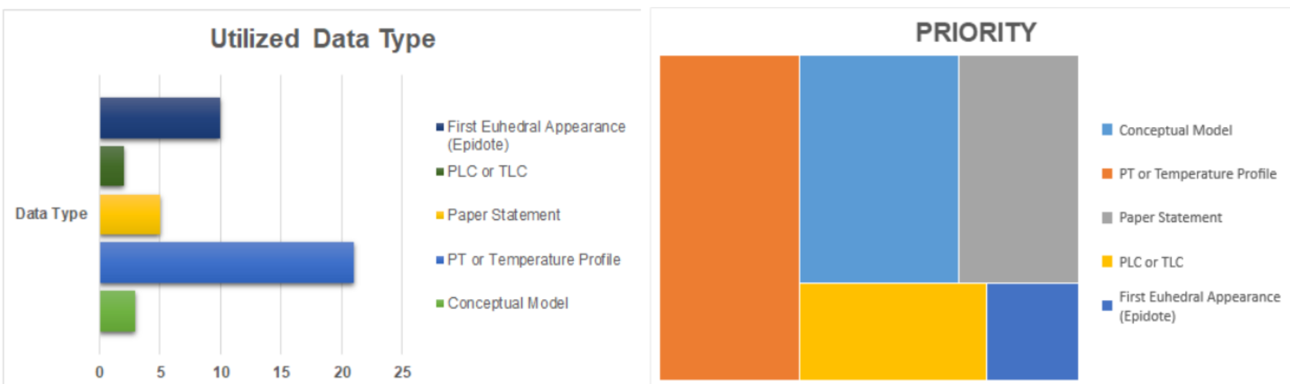

Figure 4: Utilized well-data type for actual top of reservoir information.

As shown in the hierarchical diagram, a higher confidence is favored in well data that possess natural state pressure-temperature diagrams over other utilized information.

Constraints met during data collection as shown in Figure 4 can be divided into two things, data availability and data compatibility with the software. A lot of published geothermal fields information cannot be utilized despite its play type compatibility due to lack of accessibility of the information, available information is presented in poor or difficult-to-distinguish resolution, or asynchronous available reservoir information.

No.	Well Name	Field	Geothermal System	Well Ground Elevation	BOC Elevation	Boiling Chloride Spring / None	Boiling Chloride Spring Distance (Km)	Boiling Chloride Spring Elevation	Temperature Estimate	T.o.R Elevation	Actual T.o.R Elevation (m asl)	Actual ToR Elevation Data	Sources
1	LHD-23	Lahendong	Water-dominated	900	(50)- (-400)	None	-	-	200-322 (Gas Geothermometer)	(-350) - (-1299)	-800	First epidote appearance + TLC + PLC	Rahardjo et al. (2009); Prijanto et al.(1984); Koestono (2010)
2	LHD-28	Lahendong	Water-dominated	900	0 - 50	None	-	-	200-322 (Gas Geothermometer)	(-13,8) - (-1299,2)	-250	First epidote appearance + TLC + PLC	Rahardjo et al. (2009); Prijanto et al.(1984); Koestono (2010)
3	PAD I-I	Salak	Water-dominated	900	10-300	Yes	6	200	196-256 (Silica Geothermometer)	(-306) - 253.74	200	Pressure-Temperature Profile	Aprilina et al (2017), Stimac et al, (2008)
4	RD-Y	Rantau Dadap	Water-dominated	2200	1300-1350	None	-	-	210-240 (gas geothermometer)	1086.97-1305.96	1200	Pressure-Temperature Profile	Dyaksa et al (2016), Abiyudo et al (2015)
5	ML-A1	Muara Laboh	Water-dominated	1420	750-800	Yes	5	795	182-202 (silica,Nak-K-Ca, and Na-K-Mg geothermometer)	699,59-793,52	750	Pressure-Temperature Profile	Dyaksa et al (2016), Wisnandary et al (2012)
6	LMB-1/3	Lumut Balai	Water-dominated	950	580-720	None	-	-	240-260 (Na-K-Mg geothermometer)	276.46-445.24	300	Pressure-Temperature Profile	Kamah et al (2010), Hamdani et al (2020)
7	TLG 3-1	Karaha	Vapor Dominated	1450	0-400	None	-	-	217-225 (silica, Na-K-Ca, Na-K-Mg geothermometer)	-1.95 - 38.67	25	Pressure-Temperature Profile	KESDM (2017), Powell et. al (2001); Prabata, W., and H. Berian (2017)
8	PPL-01	Patuha	Vapor Dominated	1900	1500-1550	None	-	-	220-245 (Gas Geothermometer: log (H2/H2O) vs log (H2/N2))	1197-1433	1199	Pressure-Temperature Profile	Elfina (2017); PWC et al. (2013)
9	PPL-03	Patuha	Vapor Dominated	2000	1300-1400	None	-	-	220-245 (Gas Geothermometer: log (H2/H2O) vs log (H2/N2))	1046-1281	1200	Pressure-Temperature Profile	Elfina (2017); PWC et al. (2013)
10	PPL 03 AST	Patuha	Vapor Dominated	2000	1250-1300	None	-	-	220-245 (Gas Geothermometer: log (H2/H2O) vs log (H2/N2))	997-1229	1000	Pressure-Temperature Profile	Elfina (2017); PWC et al. (2013)
11	PPL 03 BST	Patuha	Vapor Dominated	2000	1250-1350	None	-	-	220-245 (Gas Geothermometer: log (H2/H2O) vs log (H2/N2))	999-1230	1000	Pressure-Temperature Profile	Elfina (2017); PWC et al. (2013)
12	PPL 05 ST	Patuha	Vapor Dominated	2000	1250-1500	None	-	-	220-245 (Gas Geothermometer: log (H2/H2O) vs log (H2/N2))	1109-1319	1250	Pressure-Temperature Profile	Elfina (2017); PWC et al. (2013)
13	Well-29	Darajat	Vapor Dominated	1750	800-1000	None	-	-	220-237 ****	660,04 - 876,89	800	Paper statement	Intani et al. (2015)
14	F1	Darajat	Vapor Dominated	2000	1000-1100	None	-	-	230-279 ****	467,24 - 913,38	550	Paper statement	Intani et al. (2015)
15	MBE-2	Wayang Windu	Vapor Dominated	2100	1400-1800	None	-	-	295-300 ****	524,62-933,572	750	Pressure-Temperature Profile	Bogie et al., (2008); Mulyadi and Ashat (2011)
16	MBB-1	Wayang Windu	Vapor Dominated	2200	1200-1800	None	-	-	295-300 (Bogie et al., 2008)	330,34-926,4	600	Conceptual model	Bogie et al. (2008)
17	ULB-01	Ulumbu	Water-dominated	700	-50 -(-450)	None	-	-	230-240 C ****	(-212,35)- (-634,7)	-500	Pressure-Temperature Profile	Yuono and Daud (2020); Kurniawan et al. (2017); Grant et. al. (1997)
18	PT 5D	Northern Negros	Water-dominated	1000	-600-(-100)	None	-	-	260-270 (Solute geothermometer, Na-K)	(-730)- (-1032,18)	-1000	Pressure-Temperature Profile	Los Banos (2012); Zaide-Delfin et al. (1998), Dulce and Zaide-Delfin (2005); Yglopaz et al. (2005)
19	CN-3D	BacMan	Water-dominated	750	(-100) - (300)	Yes	10	5	184-271 (Solute geothermometer: Na-K)	-258 - (-635,15) masl	-450	Pressure-Temperature Profile	Tugawin et al (2015); Austria (2008); Ramos and Espartines (2015)
20	PAL 21	BacMan	Water-dominated	700	-200 - (-250)	Yes	10	5	184-271 (Solute geothermometer: Na-K)	-671 - (-870) masl	-800	Pressure-Temperature Profile	Tugawin et al (2015); Austria (2008); Ramos and Espartines (2015)
21	PAL 19D	BacMan	Water-dominated	700	-400-(-450)	Yes	10	5	184-271 (Solute geothermometer: Na-K)	-870 - (-1069)	-1000	Pressure-Temperature Profile	Tugawin et al (2015); Austria (2008); Ramos and Espartines (2015)
22	CN 2D	BacMan	Water-dominated	700	-50 -(-100)	Yes	10	5	184-271 (Solute geothermometer: Na-K)	-479 - (-766,2)	-600	Pressure-Temperature Profile	Tugawin dkk (2015); Austria (2008); Ramos and Espartines (2015)
23	RK-25	Rotokawa	Water-dominated	400	-650 - (-600)	Yes	2.6	400	183-208 (Solute Geothermometer:silica)	(-716,85) - (-607,06)	-650	Updated Conceptual Model	Sewell et al. (2012); Browne (1988).
24	RK-1	Rotokawa	Water-dominated	400	(-100) - 200	Yes	3.2	400	183-208 (Solute Geothermometer:silica)	(-844,26) - 147,13	-550	Updated Conceptual Model	Sewell et al. (2012); Browne (1988).
25	NM2	Ngatamariki	Water-dominated	350	-300-(-260)	None	-	-	180-240 (geotermometer Na-K-Mg)	(-517,83)-(-283,07)	-500	Pressure-Temperature Profile	Chambefort, (2015)
26	OW-902	Olkaria	Extensial domain type	2000	1200-2000	None	-	-	225-291 (Qtz-CO2 geothermometer)	1049,59 -1332,08	1225	First epidote appearence	Onacha (2009); Lagat (2012); Karingithi (2000)
27	OW-903	Olkaria	Extensial domain type	2000	1100-1500	None	-	-	225-291 (Qtz-CO2 geothermometer)	(-945,36) - (1055,91)	955	First epidote appearence	Onacha (2009); Lagat (2012); Karingithi (2000)
28	NJ-11	Nesjavellir	Rifting	250	(-320)-(-300)	None	-	-	200-325 **	(-1723,46)-(-327,92)	-1000	Pressure-Temperature Profile	Árnason et al (1987); Gudmundur et al (2015) , Ping (1991)
29	NJ-14	Nesjavellir	Rifting	390	(-300)-(-120)	None	-	-	197-354 **	(-2400,72)-(-294,05)	-412	First epidote appearence	Árnason and Flóvenz (1992); Nouraliee, (2000); Ping (1991)
30	NJ-15	Nesjavellir	Rifting	300	(-400)-50	None	-	-	197-354 **	(-2226,35)-(-362,72)	-500	Pressure-Temperature Profile	Árnason and Flóvenz (1992), Ping (1991), Ntihabose (2015)
31	KR-02	Krýsuvík	Rifting	100	(-250)-(-200)	None	-	-	250-330 (Gas geothermometer: H2S/Ar-H2/Ar)	(-1407,5)-(-157,76)	-637	First epidote appearence	Didana (2010), Irabaruta (2010)
32	KR-05	Krýsuvík	Rifting	100	(-225)-50	None	-	-	199-310 (Chlorite geothermometer)	(-1057,17)-(-198,61)	-550	Pressure-Temperature Profile	Didana (2010), Hogenson (2017)
33	KR-06	Krýsuvík	Rifting	100	(-400)-25	None	-	-	199-310 (Chlorite geothermometer)	(-1080,73)-(-341,39)	-800	Pressure-Temperature Profile	Didana (2010), Hogenson (2017)
34	KR-08	Krýsuvík	Rifting	200	100-150	None	-	-	250-330 **	(-1408,67)-(-163,45)	-700	Pressure-Temperature Profile	Didana (2010), Ngaruye (2009), Hogenson (2017)
35	TR-01	Trölladyngja	Rifting	150	(-400)-(-250)	None	-	-	200-280 **	(-887,88)-(-381,53)	-540	First epidote appearence	Didana, 2010; Hogenson (2017)
36	TR-02	Trölladyngja	Rifting	200	(-100)-200	None	-	-	200-280 **	(-456,51)-(-173,58)	-362	First epidote appearence	Didana, 2010; Hogenson (2017)
37	RN-09	Reykjanes	Rifting	0	(-200)-0	None	-	-	200-350 **	(-2038,44)-(-511,99)	-634	First epidote appearence	Didana, (2010); Hogenson (2017); Axelsson et al. (2015)
38	RN-10	Reykjanes	Rifting	0	(-500)-0	None	-	-	199-310 (Chlorite geothermometer)	(-968,18)-(115,97)	-600	First epidote appearence	Didana, 2010; Hogenson (2017)
39	RN-17	Reykjanes	Rifting	0	(-600)-(-200)	None	-	-	183-208 (silica Geothermometer)	(-396,33)-(-217,55)	-312	First epidote appearence	Didana, 2010; Hogenson (2017)
40	RN-20	Reykjanes	Rifting	0	(-800)-(-100)	None	-	-	183-208 (silica Geothermometer)	(-767,41)-(-128,84)	-600	First epidote appearence	Didana, 2010; Hogenson (2017)
41	34-RD2	Coso	Water-dominated	0	100-500	None	-	-	295-300 (Solute Geothermometer: Na-K-Ca)	(-777,5)-(-366,37)	-500	Paper statement	Newman et al., (2008)

Table 1: Input Parameters and Result from JIWA T.o.R. **) Geothermometer from the well sample, *) Mineral Geothermometer, *) Unknown Geothermometer Method**

5. RESULT

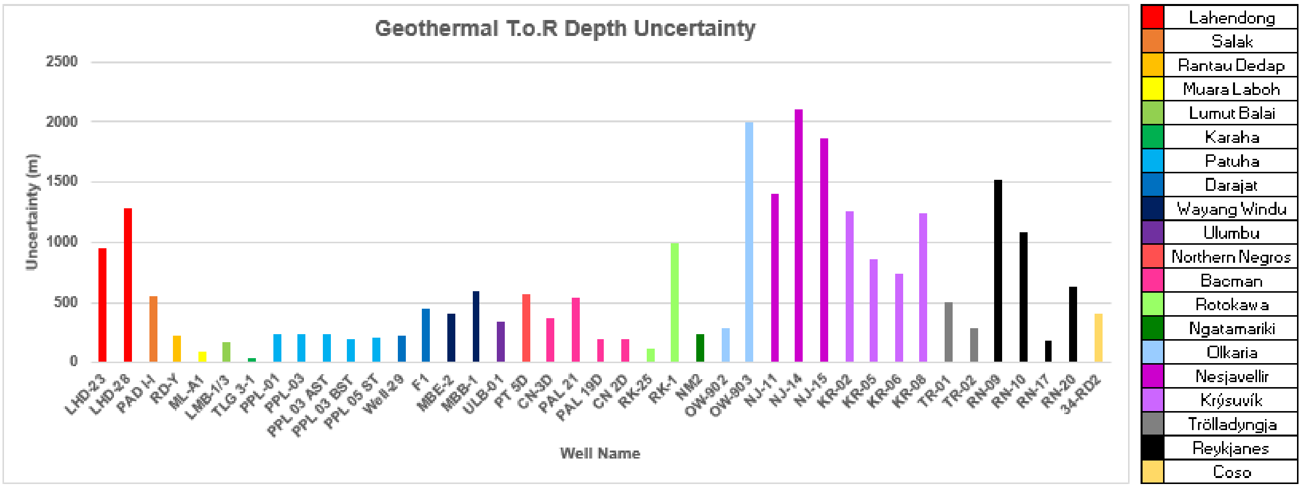

Figure 5: Geothermal T.o.R depth uncertainty of each reservoir

Figure 5 displays how reservoirs in the same geothermal field may possess different levels of uncertainty. This fact affirms how each geothermal field is unique and thus requires specialized consideration pre-drilling activity, which is by minimizing the T.o.R uncertainties.

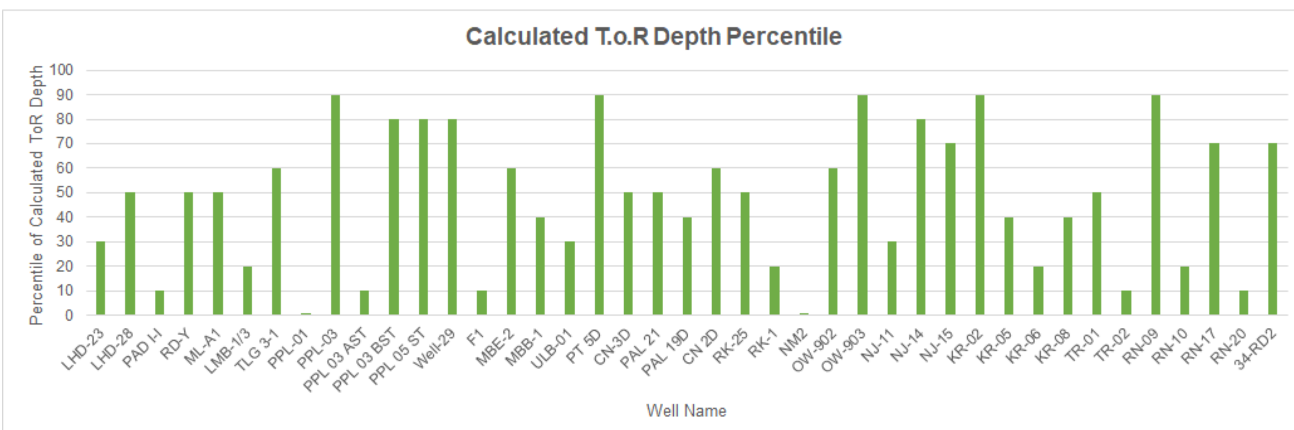

Figure 6: Calculated T.o.R depth percentile from each well

Each well's uncertainty is portrayed through measurement of the uncertainties range. It is shown that well that relies on attested conceptual models having the least uncertainty, followed by (natural state) pressure and temperature diagram, and lastly, the first euhedral appearance. The reason why conceptual models correspond with the lowest uncertainty is due to the fact that conceptual models have the least epistemic uncertainty, meaning that the data collection utilized to make the model have been more complete and integrated - hence more representative of the well condition. First euhedral appearance, on the other hand, does not lend as much confidence, especially in magmatic - vapor phase system since the occurrences are usually out of equilibrium of the thermal regime (Rejeki et al., 2010), thus no longer representing the actual site condition. The graph shows TLG 3-1 has minimum uncertainty width and RN-10 has maximum uncertainty width.

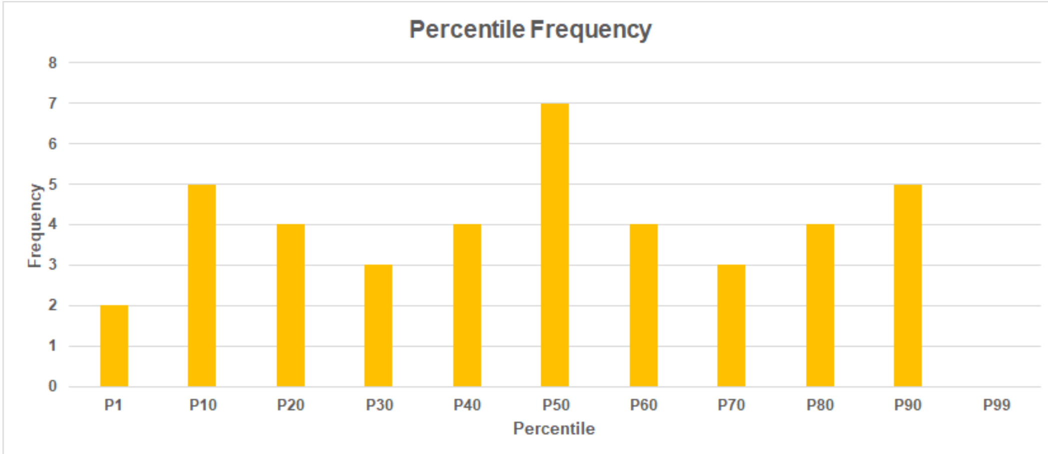

Figure 7: Frequency shows percentile distribution for overall well data

Plot of reservoir to their respective percentile calculation for T.o.R depth have displayed prevalence of the T.o.R depth is primarily found P50 (Figure 7). It means, the actual T.o.R is situated at the best (mean) estimate of JIWA T.o.R system. While this fact does not represent all worldwide conditions, it proves that the estimate calculated from JIWA T.o.R system gives the best estimate since the range corresponds with the input parameters and depicts the T.o.R coverage to determine the geothermal top of the reservoir.

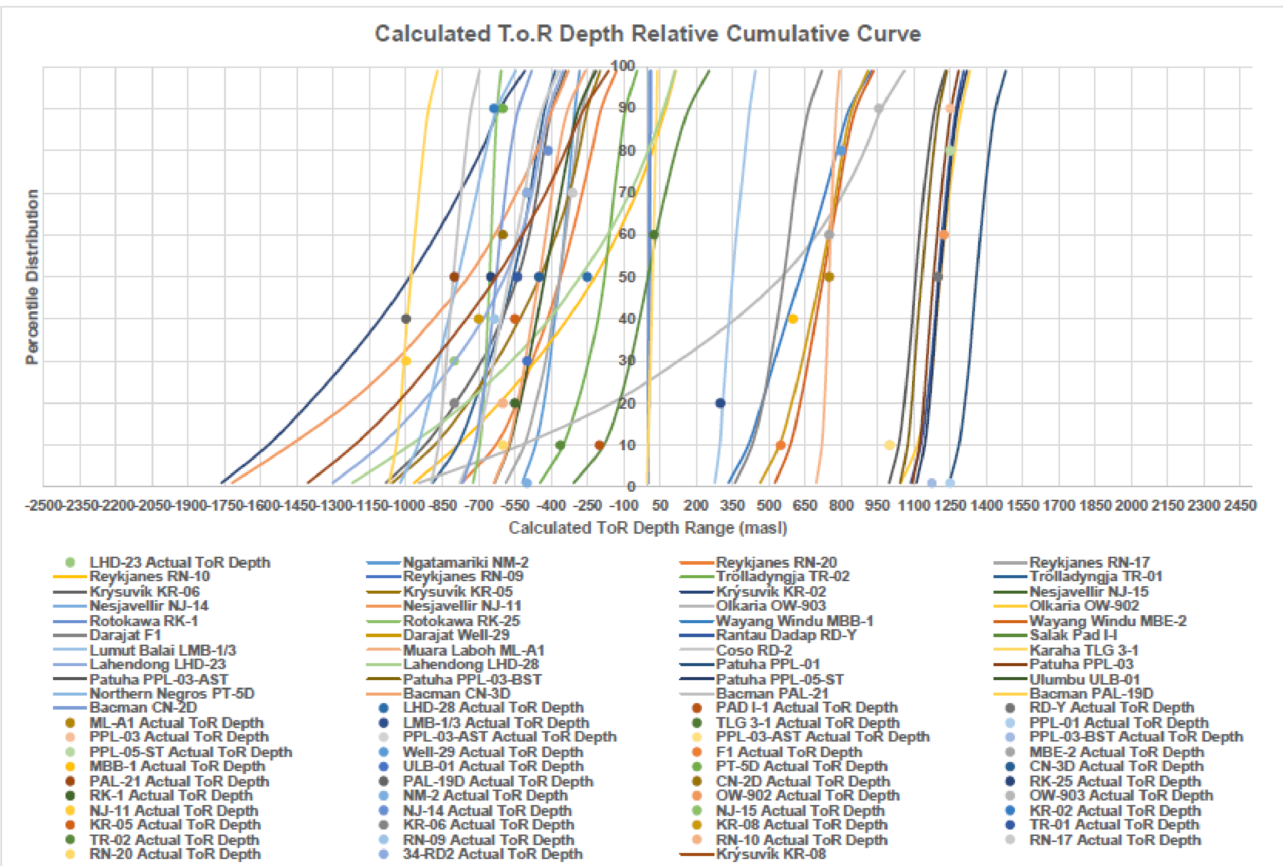

Figure 8: Relative cumulative curve from overall well data

Relative cumulative curve depicts calculated T.o.R depth range by JIWA T.o.R with actual T.o.R depth. The results vary depending on the prior well information; some well depicts a steep S-curve, indicating the uncertainty level in determining the T.o.R is minimum. Conversely, some well depicts a sloping S-curve, indicating that the uncertainty level in determining the T.o.R is bigger.

Differences in uncertainty level can be resulted due to two things: data availability for input parameters and also inherent uncertainties from the input parameter utilized to calculate the T.o.R depth range. When it concerns data availability, we are talking about reducing the epistemic uncertainty either by gaining more data collection or integrating available data from various geoscience aspects to provide a conclusive and comprehensive depiction.

From Figure 8, Karaha TLG 3-1 possesses the steepest curve and Olkaria OW-903 possesses the most sloping curve. If inferred from the input parameter utilized, it can be concluded that Karaha TLG 3-1 possesses the least epistemic uncertainty, given the B.o.C information and reservoir fluid parameters (temperature estimate) is based on conceptual models that have been updated with drilling information. On the other hand, Olkaria OW-903 possesses significant epistemic uncertainty, as the actual T.o.R information is inferred from the first epidote (euhedral) appearance (soft data).

However, when it concerns inherent uncertainties from the input parameter, the aleatory variability from the subsurface exploration data also needs to be considered, where not only geological setting but setting which parameter is more sensitive in approximating the base of conductive becomes paramount. Presented below is the sensitivity analysis by comparing relations between B.o.C elevation uncertainty to T.o.R uncertainty with temperature (input) uncertainty with the T.o.R uncertainty.

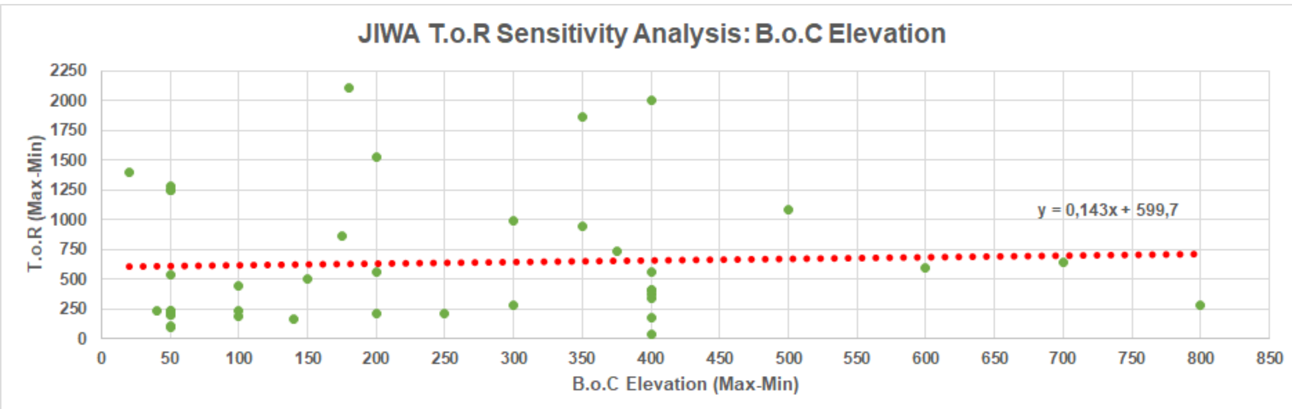

Figure 9: JIWA T.o.R sensitivity analysis - B.o.C elevation

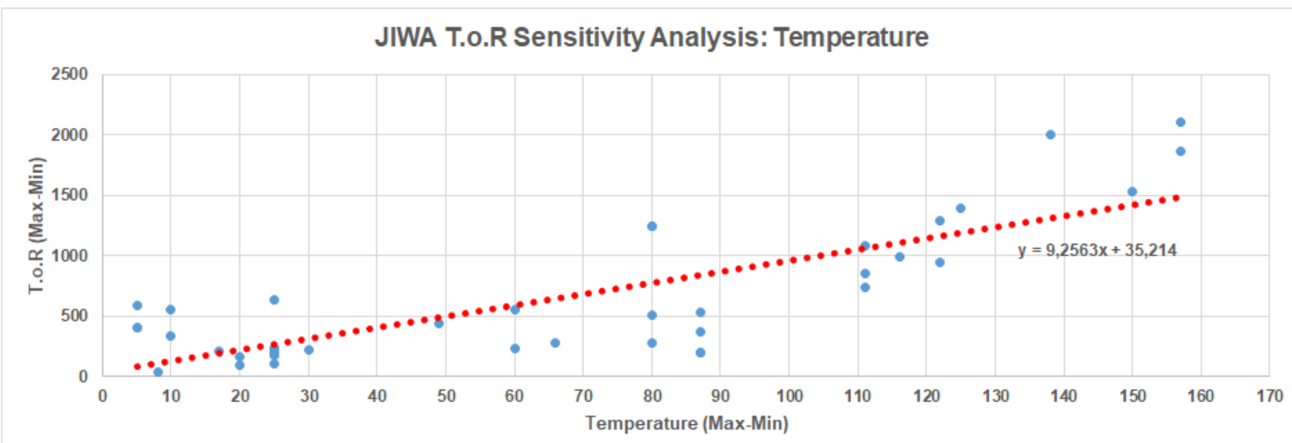

Figure 10: JIWA T.o.R sensitivity analysis – Temperature

A further uncertainties analysis from the relative cumulative curve is done by analysing whether inherent uncertainty from the base of conductive (**Figure 9**) and temperature estimate (**Figure 10**) affects the uncertainty width. Calculation results show that inherent temperature estimates' uncertainty have a higher gradient and defined trendline compared to base of conductive, thus becoming a more determining factor in reducing the top of reservoir uncertainties. Furthermore, temperature estimates obtained from silica geothermometer via boiling chloride spring have a higher probability in reducing the uncertainties since the silica geothermometer works best at 150-225^{0}C (Fournier, 1977). Moreover the study by Kuzmin (2002) shows the gas geothermometer results are more scattered than the solute geothermal result. However, the comparison can only be made between two or more reservoirs with high temperature disparity.

6. FIELD CASE

6.1 Well RK-25 (Rotokawa)

The Rotokawa geothermal field is a liquid dominated geothermal system. This field is located within the Taupo Volcanic Zone (TVZ) on the north island of New Zealand. In this study, RK-25's top of reservoir is evaluated using JIWA T.o.R. 3D-inversion MT cross-section as illustrated in Figure 11 implies that the B.o.C elevation below the well RK-25 is around -650 to -600 meter above sea level (m asl). The B.o.C has been interpreted by the low resistivity anomaly (5-10 ohm.m) that correlates to smectite clay cap. The silica geothermometer silica result from the boiling chloride spring is around 183-208^{0}C. This boiling chloride spring is located 2,6 km from the well RK-25, at an elevation of about 400 masl. The expected reservoir in RK-25 is extrapolated first from the boiling chloride spring location using horizontal geothermal gradient (5-15^{0}C/km). The expected reservoir temperature in RK-25 is around 193-247^{0}C.

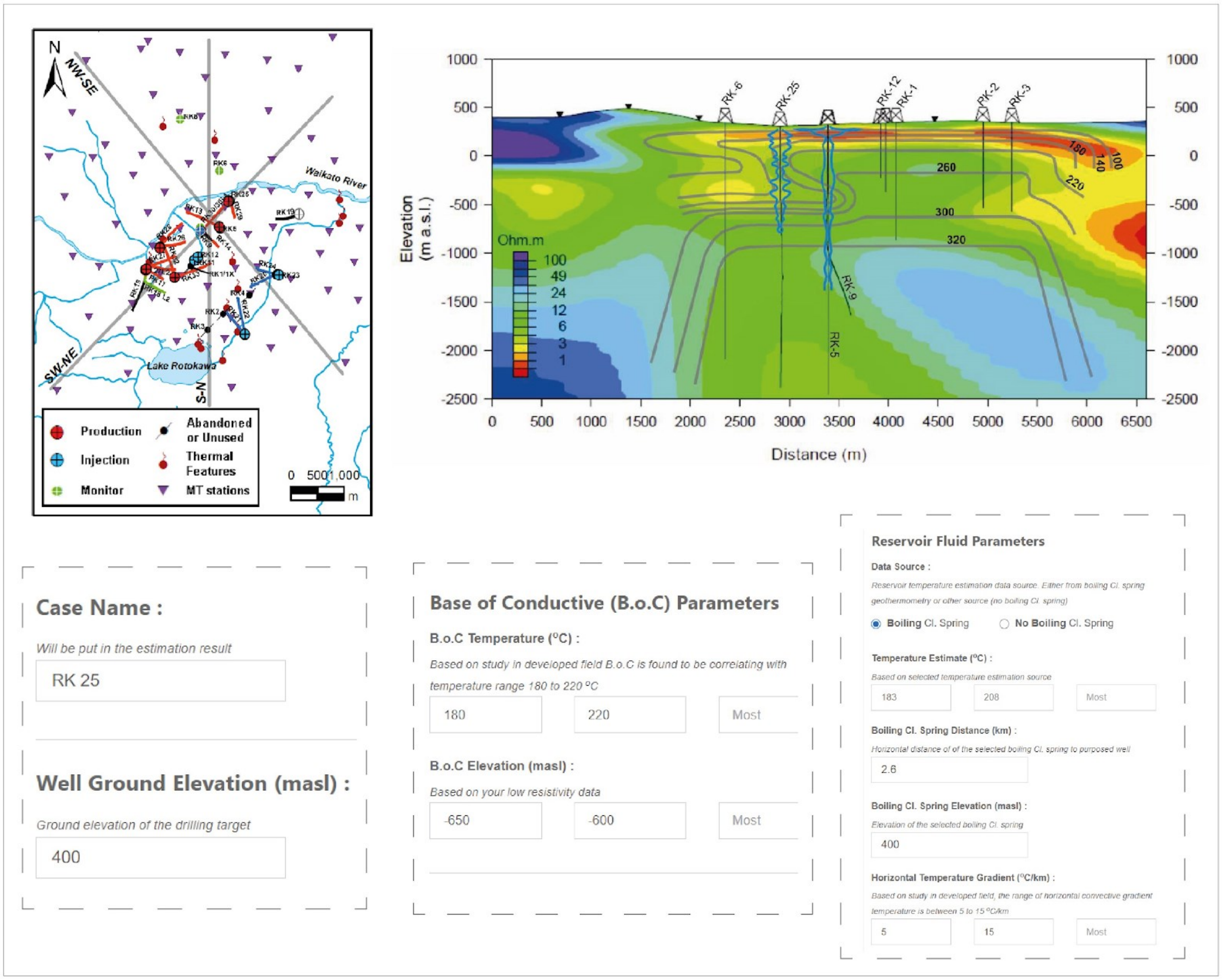

Figure 11: Input parameter from RK-25 in JIWA T.o.R. MT cross-section was obtained from Sewell et al. (2012)

In this case, we compared the actual T.o.R using the updated conceptual model by Sewell et al.(2012), the updated conceptual model shows the natural state based on measured well data, relevant geological and physical information (**Figure 12**). The top of the reservoir from the updated conceptual model is expected around -600 m asl.

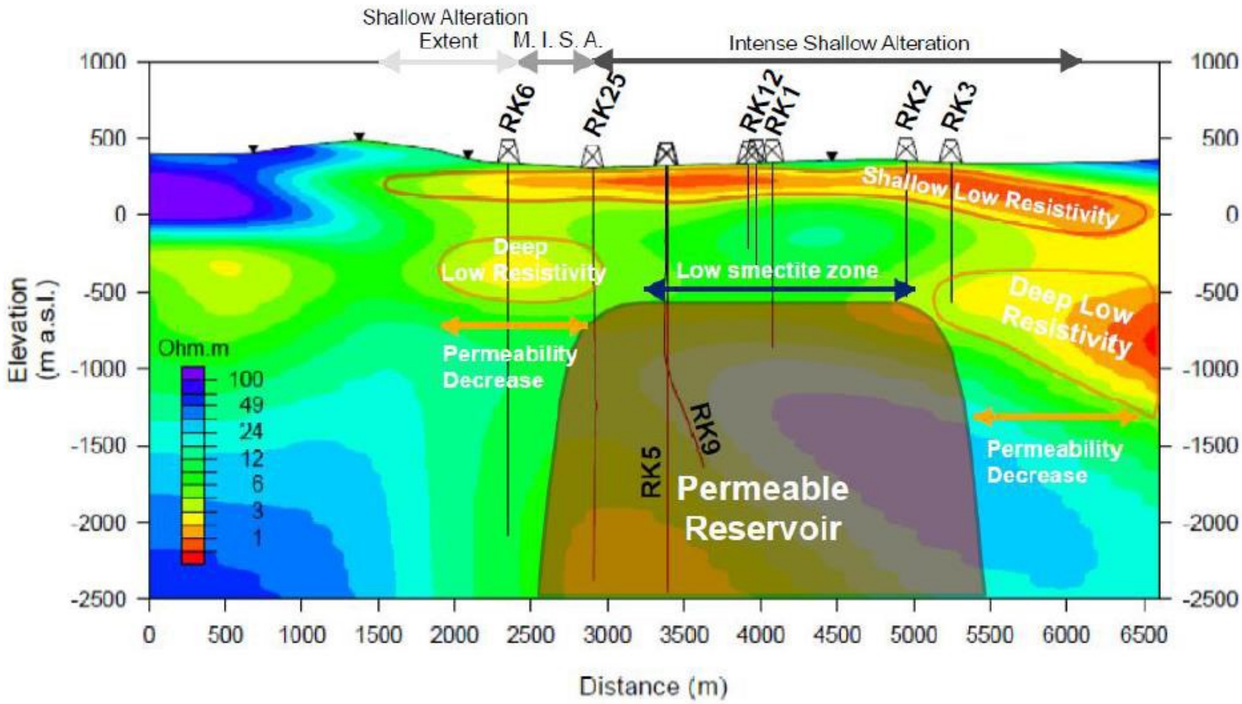

Figure 12: Conceptual model to confirm the top of reservoir derived from a 3-D MT cross-section N-S (Sewell et al., 2012).

The JIWA T.o.R estimation result of well RK-25 shows the T.o.R uncertainties in a range of ± -607 to -721 m asl (**Figure 12**) that correlated with the P50 of JIWA T.o.R estimation **(Figure 13**).

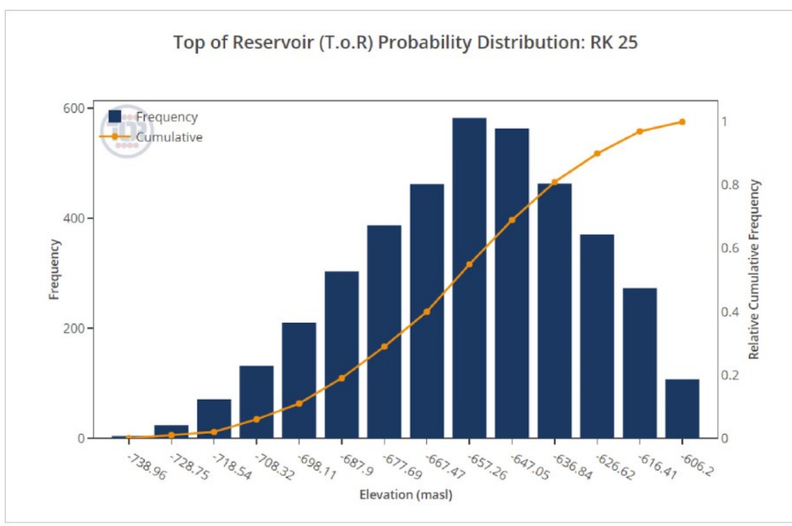

Figure 13: Histogram of Well RK-25 T.o.R probability distribution

Rotokawa RK-25	
Percentile	T.o.R Elevation (masl)
P1	-722,77
P10	-694,21
P20	-680,49
P30	-671,06
P40	-662,55
P50	**-654,78**
P60	-647,58
P70	-640,55
P80	-632,75
P90	-623,15
P99	-607,08

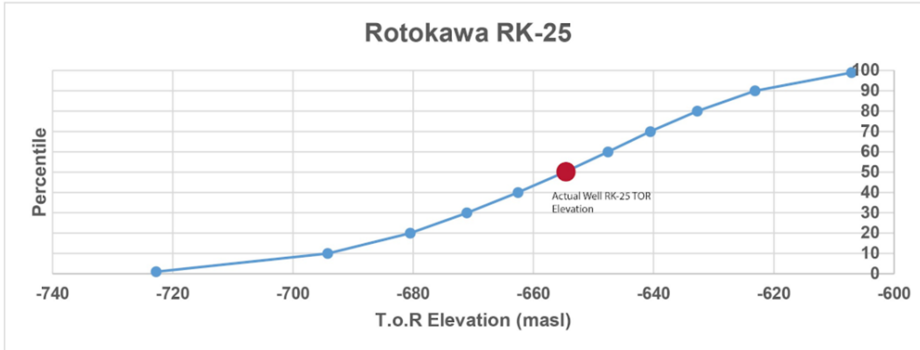

Figure 14: JIWA T.o.R result for RK-25, Rotokawa

6.2 Well PPL-03-BST (Patuha)

The Patuha geothermal field is located in Bandung and Cianjur Districts, West Java Province, Indonesia. The B.o.C elevation below well PPL-03-BST is interpreted around 1,250-1,350 m asl based on the low resistivity in the cross section of MT shown in Figure 16. The study about reservoir temperature by PWC et al. (2013) shows the reservoir temperature expected around 220-240°C using gas geothermometers (log (H2/H2O) vs log (H2/N2).

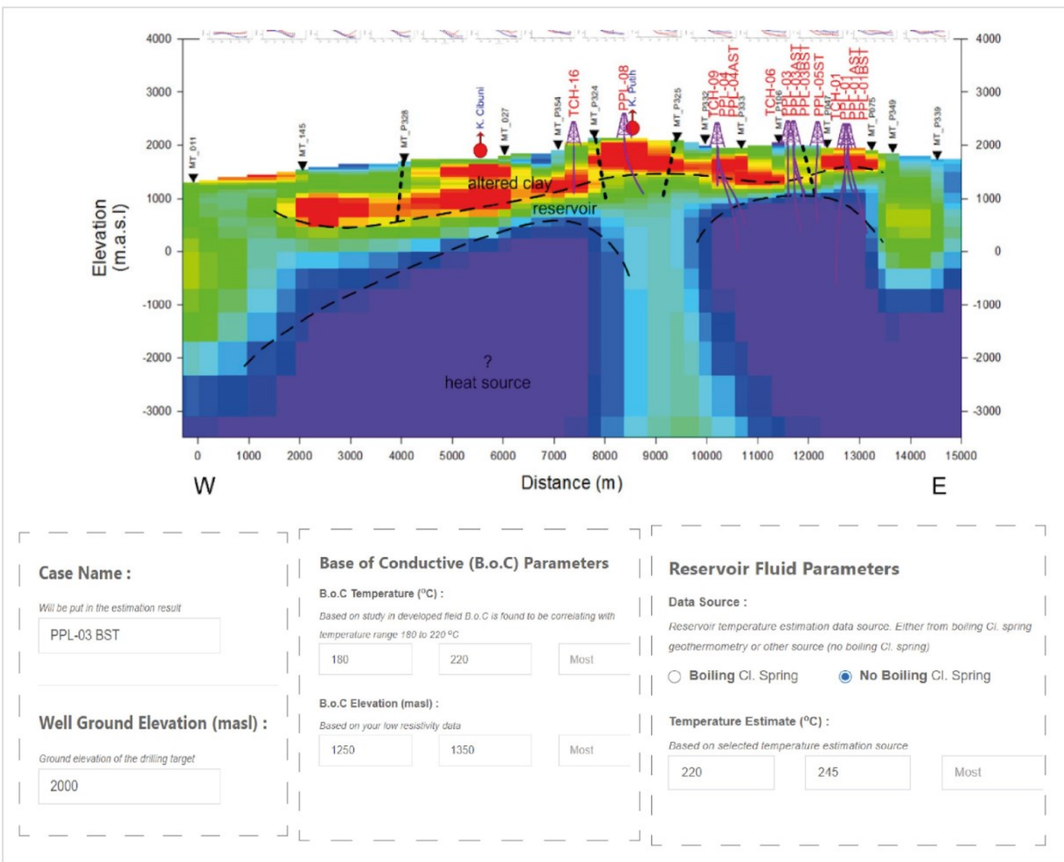

Figure 15: Input parameter PPL-03-BST in JIWA T.o.R. MT cross-section is obtained from Elfina (2017)

The actual reservoir was identified by the convective zone of the temperature profile. Convective profiles can be described by isothermal sections. An isothermal profile is a part of the well where the temperature and depth are constant or almost constant with depth. The actual well PPL-03 BST top of the reservoir is ±1,175 m asl (**Figure 8**).

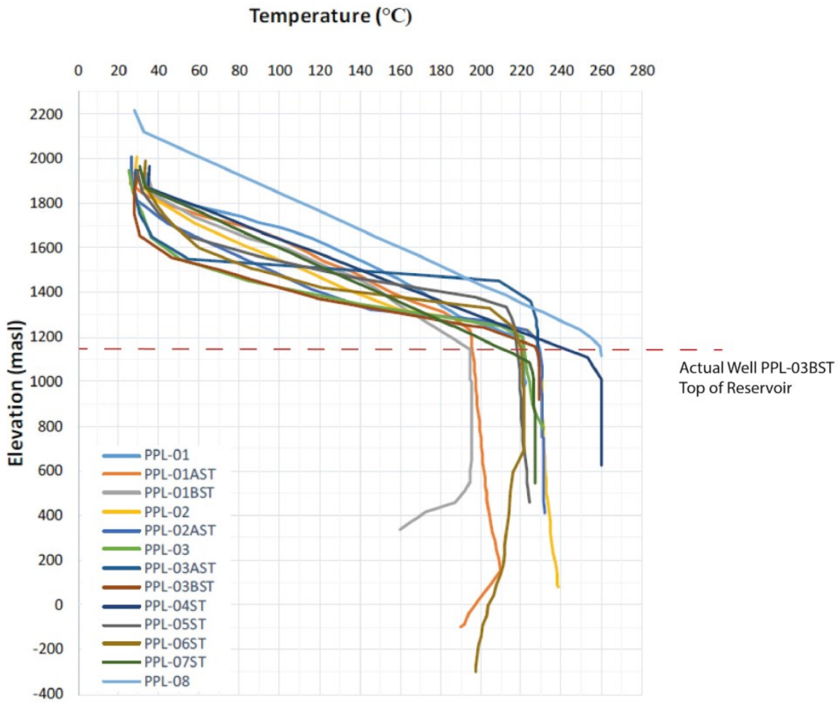

Figure 16: Well PPL-03 BST actual top of reservoir from the temperature profile (Elfina, 2017)

The JIWA T.o.R estimation result shows the T.o.R uncertainties in a range of ± -1,038 to -1,240 m asl. The actual top of reservoir correlated with the P80 of JIWA T.o.R estimation (**Figure 16**).

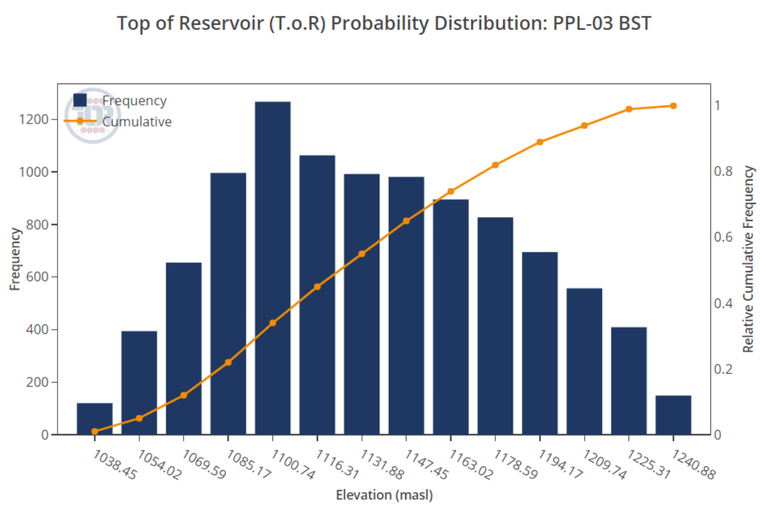

Figure 17: Histogram of Well PPL-03-BST for T.o.R probability distribution

Patuha PPL-03-BST	
Percentile	T,o,R Elevation (masl)
P1	1044,16
P10	1074,17
P20	1091,56
P30	1104,67
P40	1118,1
P50	1133,53
P60	1148,99
P70	1164,54
P80	**1182,71**
P90	1204,83
P99	1236,58

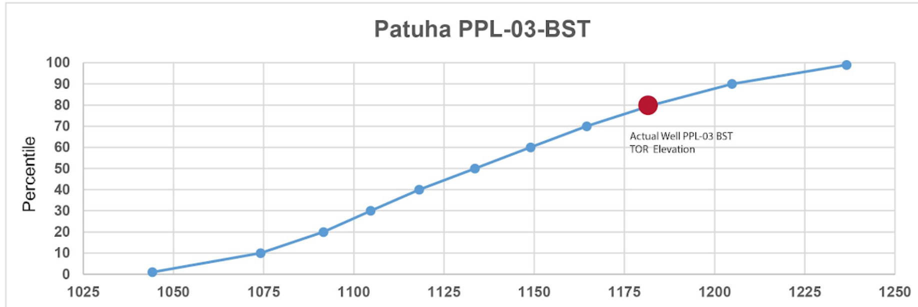

Figure 18. JIWA T.o.R result for PPL-03-BST, Patuha

These two fields have a distinguished characteristic, the presence of the boiling chloride spring and no boiling chloride spring, shows a different result. Well RK-25 with the boiling chloride spring has a lower degree of uncertainty than Well PPL-03-BST. The higher uncertainty of the well PPL-03-BST is affected by the higher range of the BOC elevation (1250-1350 m asl) than well RK-25 ((-650)-(-600)) m asl. These results prove that B.o.C elevation inherent uncertainty plays a significant role in influencing the T.o.R depth uncertainty. Given the similar temperature range derived from the geothermometer, the estimated reservoir temperature uncertainty is not as pronounced in influencing the T.o.R depth uncertainty.

7. CONCLUSION

Forty-one geothermal wells from all over the world comprising both vapor and liquid-phase geothermal systems have been analysed within this study, showing how JIWA T.o.R successfully covers all depth uncertainties. It is concluded how P-T diagrams and conceptual models possess higher confidence since their (epistemic uncertainty) have reduced due to integration of drilling data, and further proven from the T.o.R range results. Data visualization depicts how temperature estimates derived from geothermometer data as one of the input parameters more significantly influence the T.o.R uncertainty rather than B.o.C elevation information derived from the resistivity model. This claim is proven by the sensitivity analysis that shows higher gradients for the temperature uncertainty, thus becoming a more determining factor in reducing T.o.R uncertainties. Furthermore, temperature estimates obtained from silica geothermometer via boiling chloride spring have a higher probability in reducing the uncertainties. However, when a comparative of two or more reservoirs are made with similar temperature range, the B.o.C elevation uncertainty is much more pronounced compared to the temperature one. Nevertheless, the calculation results prove that both B.o.C elevation and temperature estimate are crucial in constraining T.o.R uncertainties to reduce drilling risks.

REFERENCES

Abiyudo, Rizal, Julfi Hadi, Dayinta Adi Dyaksa Alfiady, and Tom Powell: The Understanding of Gas Geochemical Model to Reduce the Exploration Risk; A Case Study in Rantau Dedap. *Proceedings,* Indonesia International Geothermal Convention & Exhibition, (2015).

Adams A. J. et al: Probabilistic Well Time Estimation Revisited, SPE/IADC 119287 presented at the SPE/IADC Drilling Conference and Exhibition in Amsterdam, (2009).

Adomian, G, Malakian, K.:Inversion of stochastic partial differential operators: the linear case, J. Math. Anal, **77**, (1980), 309-327.

Anderson, E., Crosby, D., Ussher, G.: Bulls-Eye! – Simple Resistivity Imaging to Reliably Locate the Geothermal Reservoir, *Proceedings,* World Geothermal Congress, Kyushu - Tohoku, Japan (2000).

Anette K. Mortensen, Ásgrímur Guðmundsson, Benedikt Steingrímsson, Freysteinn Sigmundsson, Guðni Axelsson, Halldór Ármannsson, Héðinn Björnsson, Kristján Ágústsson, Kristján Sæmundsson, Magnús Ólafsson, Ragna Karlsdóttir, Sæunn Halldórsdóttir og Trausti Hauksson: The Krafla Geothermal System Research summary and conceptual model revision, Landsvirkjun, (2015).

Aprilina, Nur Vita, Fanji Junanda Putra, Satrio Wicaksono, Tri Julinawati, Reka Tanuwidjaja, and Aditya Hernawan:"Results of II Deep Well: Impact on the Conceptual Model of the Salak Geothermal System." *Proceedings (*2017).

Árnason, K., Haraldsson, G.I., Johnsen, G.V., Thorbergsson, G., Hersir, G.P., Saemundsson, K., Georgsson, L.S., Rögnvaldsson, S.Th., and Snorrason, S.P.: Nesjavellir-Ölkelduháls, surface exploration 1986. Orkustofnun, Reykjavík, report OS-87018/JHD-02 (in Icelandic), 112 pp + maps, (1987)

Austria Jr, Jaime Jemuel C.: Production capacity assessment of the Bacon-Manito geothermal reservoir, Philippines." *United Nations University, Geothermal Training Programme*, (2008).

Axelsson, G and Franzson, H.:Geothermal drilling targets and well siting. Proceedings of the “Short Course on Geothermal Development and Geothermal Wells”, organized by UNU-GTP and LaGeo, Santa Tecla, El Salvador, (2012), 16 pp.

Bogie, I., Yudi Indra Kusumah and Merry C. Wisnandary: Overview of the Wayang Windu geothermal field, West Java, Indonesia, *Geothermics,* **37,** (2008): 347-365.

Browne, P.R.L: Exploration of the Rotokawa geothermal field, Taupo Volcanic Zone, New Zealand.

Chambefort, Isabelle & Buscarlet, Etienne & Wallis, Irene & Sewell, Steven & Wilmarth, Maxwell: Ngatamariki Geothermal Field, New Zealand: Geology, geophysics, chemistry and conceptual model. *Geothermics.* 59. 10.1016/j.geothermics.2015.07.011, (2015).

Cumming, W., & Mackie, R. Resistivity imaging of geothermal resources using 1D, 2D and 3D MT inversion and TDEM static shift correction illustrated by a Glass Mountain case history. In *Proceedings world geothermal congress*, Bali, Indonesia, (2010). 25-29.

Cumming, W.: Resource Conceptual Model of Volcano – Hosted Geothermal Reservoirs for Exploration Well Targeting and Resource Capacity Assessment: Construction, Pitfalls, and Challenges, *GRC Transactions,* **40**, (2016). 623-638.

Didana, Y.: Multidimensional Inversion of MT data from Krýsuvík High Temperature Geothermal Field, SW Iceland, and study of how 1D and 2D inversion can reproduce a given 2D/3D resistivity structure using synthetic MT data, (2010).

Dyaksa, D.A., Ramadhan, I., Ganefianto, N.: Magnetotelluric Reliability for Exploration Drilling Stage: Study Cases in Muara Laboh and Rantau Dedap Geothermal Project, Sumatera, Indonesia, *Proceedings,* 41st Workshop on Geothermal Reservoir Engineering, Stanford University, Stanford, CA (2016).

Dulce, Rosella G., and Maribel C. Zaide-Delfin.: Exploration and Delineation Drilling in a High-Temperature Geothermal Reservoir: Northern Negros Geothermal Field, Central Philippines. In *Proceedings of the World Geothermal Congress*, (2005), 24-29

Elfina: Updated Conceptual Model of The Patuha Geothermal Field, Indonesia, (2017).

Essene, E. J., & Peacor, D. R.: Clay mineral thermometry—a critical perspective. *Clays and clay minerals*, ***43***, (1995). 540-553.

Flóvenz, Ó.G., Georgsson, L.S., and Árnason, K: Resistivity structure of the upper crust in Iceland, J. Geophys. Res., 90-B12, 10,136-10,150, (1985).

Fournier, R. O.: Chemical geothermometers and mixing models for geothermal systems. *Geothermics*, (1977), 41-50.

Grant, M. A., H. Hole, M. Melaku, and PT. PLN.:Efficient Well Testing at Ulumbu Field, Flores, Indonesia." In *Proceedings of 22nd Workshop on Geothermal Reservoir Engineering Stanford University, California, USA*, (1997).

Grant, M.A., and Bixley, P.F.: Geothermal Reservoir Engineering 2nd Edition, *Elsevier* (2011).

Gudmundur, Omar & Friðleifsson, G.Ó & Albertsson, Albert: Deep geothermal drilling on the Reykjanes ridge opportunity for international collaboration. Proceedings of the World Geothermal Congress, (2000).

Gunderson, G., Harvey, C., Johnstone, R., Anderson E.: Analysis of Smectite Clays in Geothermal Drill Cuttings by the Methylene Blue Method.: for Well Site Geothermometry and Resistive Sounding Correlation, *Proceedings,* World Geothermal Congress, Kyushu - Tohoku, Japan (2000).

Gylfadóttir, S. S., S. Halldórsdóttir, A. Arnaldsson, H. Ármannsson, K. Árnason, G. Axelsson, G. M. Einarsson: Revision of the conceptual model of the Greater Olkaria geothermal system-phase I. Mannvit, *ÍSOR/Vatnaskil/Verkís Consortium, report, Reykjavík,* (2011).

Hadi, Julfi, et al. "Resource risk assessment in geothermal greenfield development; an economic implications. *Bali: Proceedings World Geothermal Congress*. (2010)

Hamdani, Muhamad Ridwan, and Heru Berian Pratama: Updating the Conceptual Model of Lumut Balai Geothermal Field, South Sumatera, Indonesia Using Numerical Simulation." *In IOP Conference Series:* Earth and Environmental Science, **417**, no. 1, p. 012023. IOP Publishing, (2020).

Hogenson, J.: Geothermal Surface Mapping and Chemical Sampling in Krýsuvík at: Seltún, Trölladyngja, and Austurengjar, (2017).

Hole, H.: Geothermal well design-casing and wellhead. In Petroleum Engineering Summer School Workshop, **26**, (2008)

Hossein-Pourazad, H.:High-temperature geothermal well design. United Nations University (2005).

Intani, Rindu & Simatupang, Christovik & Sihombing, Amsal & Irfan, Riki & Golla, Glenn & Pasaribu, Fernando: West Edgefield Evaluation of the Darajat Geothermal Field, Indonesia, (2015).

Irabaruta, Constantin: Joint 1-D Inversion Of TEM And MT Resistivity Data, Comparison With Mineral Alteration And Temperature In Drillholes – Case Study: Krýsuvík Area, Sw-Iceland, (2010).

Kalos, M.V. and Whitlock, P.A.:Monte Carlo Methods, Willey-Blackwell,(2008)

Kamah, M. Y., D. B. Hartanto, and M. H. Thamrin:The evidence used in targeting wells in a geothermal reservoir using fracture zones and erratic structure at Lumut Balai and Tompaso Geothermal Area, Indonesia." *Proceedings*, World Geothermal Congress 2010 (2010).

Karingithi, Cyrus W: Geochemical characteristics of the Greater Olkaria geothermal field, Kenya, (2000).

KESDM:Potensi Panas Bumi Indonesia Jilid 1, (2017)

Koestono, H.: Lahendong Geothermal Field, Indonesia: Geothermal model based on wells LHD-23 and LHD-28. United Nations University, Geothermal Training Programme, (2010).

Kurniawan, Iqbal & Sutopo, Topo & Pratama, Heru:. A Natural State Modelling Of Ulumbu Geothermal Field, East Nusa Tenggara, Indonesia, (2017).

Kuzmin, Dmitry.:Solute and gas geothermometers. United Nations University, (2002).

Lagat, John: Hydrothermal alteration mineralogy in geothermal fields with case examples from Olkaria Domes geothermal field, Kenya, (2012).

Los Banos, C. E. F.: Three-Dimensional Magnetotelluric (MT) Modeling of the Northern Negros Geothermal Project, Central Philippines, (2012).

Mason, Colin J., Jesse Lopez, Sigve Meling, Robert Munger, and Barry Fraser: Casing Running Challenges for Extended-Reach Wells." In *SPE Annual Technical Conference and Exhibition*. Society of Petroleum Engineers, (2003).

Mahagyo, R. Purwantoko, P. Molling and Abu Dawud Hidayaturrobi: Baseline Geochemical Model and the Impact of Production at the Darajat Geothermal Field, Indonesia, (2009).

Makuk, Isaac Kipkoech: Reducing geothermal drilling problems to improve performance in Menengai. *UNU-GTP, Report* **16** (2013), 325-58.

Muffler, L. JP.: Tectonic and hydrologic control of the nature and distribution of geothermal resources. *Geo-Heat Center Quarterly Bulletin;(United States)* ***15***, no. 2 (1993).

Mulyadi and Ashat, Ali: Reservoir modelling of the northern vapor-dominated two-phase zone of the Wayang Windu geothermal field, Java, Indonesia, (2011).

Newman, Gregory & Gasperikova, Erika & Hoversten, G. & Wannamaker, Philip: Three-dimensional magnetotelluric characterization of the Coso geothermal field. Geothermics. 37. 369-399. 10.1016/j.geothermics.2008.02.006, (2008).

Ngaruye, Jean-Claude: Geological and geothermal mapping of Slaga-Arnarvatn area, Reykjanes Peninsula, SW-Iceland. Geothermal Training in Iceland, (2009).

Nicholson, K.: Geothermal Fluids, *Springer Verlag,* (1993).

Nouraliee, Javad: Borehole geology and hydrothermal alteration of well NJ-20, Nesjavellir high-temperature area, SW-Iceland, (2000).

Ntihabose, L.:Well test analysis and temperature and pressure monitoring of Krafla and Nesjavellir high-temperature geothermal fields, Iceland, (2015).

Omenda, P. A., S. A. Onacha, and W. J. Ambusso: Geological setting and characteristics of the high temperature geothermal systems in Kenya." In Proceedings of the New Zealand Geothermal Workshop, **15**, (1993), pp. 161-167.

Onacha, S.A. & Shalev, Eylon & Malin, Peter & Leary, Peter: Joint geophysical imaging of fluid-filled fracture zones in geothermal fields in the Kenya rift valley. Transactions - Geothermal Resources Council. 33. 465-471, (2009).

Paté-Cornell ME: Uncertainties in risk analysis: Six levels of treatment. Reliability Engineering and System Safety, v. 54, (1996), p. 95–111. doi: 10.1016/S0951-8320(96)00067-1

Petrică, V. C.: Common Geothermal Well Design and A Case Study of The Low-Temperature Geothermal Reservoir in Otopeni, Romania (2016).

Ping, Zhao: Gas geothermometry and chemical equilibria of fluids from selected geothermal fields, UNU Geothermal Training Programme, Orkustofnun - National Energy Authority, Report 14, (1991).

Powell, T., Moore, J., DeRocher, T., McCulloch, J.: Reservoir Geochemistry of The Karaha -Telaga Bodas Prospect, Indonesia. Geothermal Resources Council Transactions, **25**, (2001).

Prabata, W., and H. Berian: 3D natural state model of Karaha-Talaga Bodas Geothermal Field, West Java, Indonesia, *Proceedings,* 39th New Zealand Geothermal Workshop, (2017).

Prijanto, A. F., Lubis, L. I., & Suwana, A.: Geochemistry of the Minahasa geothermal prospect, North Sulawesi, (1984).

PWC, ELC, Hadiputranto, Hadinoto & Partners, and Mandiri Sekuritas.: Final report - consultant's services for the development of the Dieng geothermal area units 2 & 3 and Patuha units 2& 3. PT Geo Dipa Energi (Persero), Indonesia, internal report, (2013).

Ramos, Miguel Eduardo S., and Christine Marie R. Espartinez:The bacon-manito surface thermal features–geochemical and physical changes after three decades (1983-2013) of monitoring." In *Proceedings World Geothermal Congress 2015*. (2015).

Raharjo, I.B., Timisela, D.P., and Arumsari, A.F.: 3D inversion of Lahendong geothermal field. Pertamina, internal electronic file, (2009).

Rejeki, S., D. Rohrs, Gregg Nordquist and Agus Fitriyanto: Geologic Conceptual Model Update of the Darajat Geothermal Field, Indonesia, (2010).

Sarmiento, Z.: A snapshot of the drilling and completion practices in high temperature geothermal wells in the Philippines. *In*: Workshop 4 of the Engine Drilling cost effectiveness and feasibility of high-temperature drilling, Reykjavik, Iceland, (2007).

Sewell, S., W. Cumming, L. Azwar and C. Bardsley: "Integrated MT and Natural State Temperature Interpretation for a Conceptual Model Supporting Reservoir Numerical Modelling and Well Targeting at The Rotokawa Geothermal Field, New Zealand." (2012).

Sidqi, M., Situmorang, J., Harry, M., Nainggolan T.: JIWA T.o.R: Estimation of Geothermal Top of Reservoir Uncertainties in the Exploration Phase. *Forthcoming Proceedings,* 46th Workshop on Geothermal Reservoir Engineering, Stanford University, Stanford, CA (2021).

Steingrimsson, Benedikt: Geothermal well logging: Temperature and pressure logs. *Tutorial-Geothermal Training Programme* (2013).

Stimac, James, Gregg Nordquist, Aquardi Suminar, and Lutfhie Sirad-Azwar. "An overview of the Awibengkok geothermal system, Indonesia." *Geothermics,* **37**, no. 3 (2008), 300-331.

Tugawin, Randy J., David M. Rigor Jr, Carlos Emmanuel F. Los Baños, and Domingo B. Layugan: Resistivity Model Based on 2D Inversion of Magnetotelluric Sounding Data in Bacon-Manito, Southern Luzon, Philippines. In *Proceedings*. (2005).

Trainor-Guitton WJ, Hoversten GM, Nordquist G, Intani R.: Value of MT inversions for geothermal exploration: accounting for multiple interpretations of field data & determining new drilling locations. *Geothermics*, **66**, (2017),13–22.

Ussher, G., Harvey, C., Johnstone, R., & Anderson, E.: Understanding the resistivities observed in geothermal systems. In *proceedings world geothermal congress*, Kyushu, (2000). Wisnandary, C. M., Ontowiryo Alamsyah, and Supreme Energy. "Zero generation of muara laboh numerical model: role of heat loss and shallow wells data on preliminary natural state modeling." *GRC Transactions* **36** (2012): 825-830.

Witter JB, Trainor-Guitton WJ, Siler DL Uncertainty and risk evaluation during the exploration stage of geothermal development: A review. Geothermics,**78**, (2019), 233-242.

Yglopaz, David M., Ramonchito Cedric M. Malate, Arthur E. Amistoso, Arvin R. Aqui, Raymundo G. Orizonte, and Dennis R. Sanchez.: Field Management Strategies for the Developemnt of the Northern Negros Geothermal Field, Philippines." In *Proc.: World Geothermal Congress*. (2005).

Yock, A.: Geotermometry. Short Course on Surface Exploration for Geothermal Resources in Ahuachapan and Santa Tecla, El Salvador, (2009). 17-30.

Yuono, R. T., and Y. Daud: Reservoir simulation of Ulumbu geothermal field using TOUGH2 and ITOUGH2 simulator, In *IOP Conference Series: Earth and Environmental Science*, IOP Publishing, **538**, (2020).

Zabalza-Mezghani I, Manceau E, Feraille M, Jourdan A.: Uncertainty management: From geological scenarios to production scheme optimization. Journal of Petroleum Science and Engineering, **44**, (2004),11-25.

Zaide-Delfin, M. C.: R. G. Dulce, and J. A. Esperidion. "Geologic Model of the Northern Negros Geothermal Reservoir, Central Philippines." *TRANSACTIONS-GEOTHERMAL RESOURCES COUNCIL*, (1998): 95-100.